PCCP

Cite this: *Phys. Chem. Chem. Phys.*, 2011, **13**, 20100–20103

www.rsc.org/pccp

COMMUNICATION

Controlling the wall thickness and composition of hollow precipitation tubes†

László Roszol and Oliver Steinbock*

Received 8th August 2011, Accepted 26th September 2011
DOI: 10.1039/c1cp22556a

We investigate the growth of self-organized tubes formed by injection of metal salt solutions into silicate solution. The wall thickness increases strictly in an inward direction and obeys square root functions suggesting the presence of a traveling reaction-diffusion front in the radial direction. We also demonstrate the construction of multi-layered tubes.

The synthesis of materials far from thermodynamic equilibrium is a widely uncharted area of chemistry.[1] While examples are abundant in biology,[2] man-made efforts are severely limited by the problem of maintaining a reaction in a nonequilibrium state while simultaneously extracting desired products. In the case of molecular and colloidal substances, this task can often be accomplished with continuous stirred-tank reactors.[3] For solids, however, unconventional approaches are needed which typically rely on self-propagating reaction fronts.

Front-mediated reactions can produce materials with advantageous microscopic characteristics (*e.g.* frontal polymerization) as well as surprising macroscopic shapes such as hollow precipitation tubes.[4–9] The latter structures have diameters in the range of 1 μm to 1 cm. They form in a self-propagating ring-shaped reaction zone. Within this zone an exterior solution mixes and reacts with a second solution from the tube's interior. The latter reactant is continuously supplied from a source at the tube's base. In the case of the prototypical 'silica garden' experiment[6] the source is a metal salt particle and the second reactant is an aqueous solutions of sodium silicate. Numerous chemical variations of this experiment have been reported including borate, carbonate,[7] and phosphate-based[8] precipitation reactions as well as corrosion processes[4] and polyoxometalate reactions.[9] In most of these systems, the tube wall is several micrometres thick and has compositional gradients in radial direction.[4,10–12] Related features of the wall can include hierarchical nano-to-macroscale architectures,[13] high catalytic activity,[14] and photoluminescence.[15]

The tube diameter can be controlled by pinning a gas bubble to the leading reaction zone. This templating process yields very straight, high-aspect ratio tubes and could allow doping of the material.[10,16] During synthesis the structures can be permanently bent by applying weak electric fields.[17] Moreover naturally occurring precipitation tubes are possibly relevant to the formation of life because complex prebiotic chemistry could have been fueled by pH gradients across the catalytically active tube wall.[18] Unfortunately only few studies have attempted to analyze tube growth quantitatively. Exceptions include work on the selection of the outer tube radius (in the absence of bubbles)[19] and certain oscillatory features in the growth dynamics.[20,21]

Herein we report a method for increasing and controlling the wall thickness of precipitation tubes. The approach is demonstrated for structures formed in silicate solution but should also be applicable to other systems. Moreover it yields quantitative insights into the growth dynamics suggesting that radial wall growth is driven by a unidirectional reaction-diffusion front.

In our experiments we inject either aqueous $CuSO_4$ or $ZnSO_4$ solution (0.5 M) through a nozzle into a glass cylinder filled with sodium silicate solution at concentrations of 1.0, 1.5, or 2.0 M. At the nozzle we introduce a single air bubble that attaches to the nucleating tube. It remains pinned during the vertical growth process (Fig. 1a) generating a very straight tube of a constant outer radius R. This radius is only slightly smaller than the bubble radius. The vertical growth velocity v is determined by R and the volume flow rate Q of the injected reactant A according to $v = Q/(\pi R^2)$.[10] For our flow rate of $Q = 4.0$ ml h^{-1}, this yields $v = 0.67$ cm s^{-1} which is in good agreement with our observations. Accordingly the tube reaches the meniscus of the 10 cm high silicate reservoir within 15 s.

At the end of this initial phase (in the following $t = 0$) the slightly translucent structures are light blue ($CuSO_4$ injection) or white ($ZnSO_4$ injection). We then continue the injection of A at the same flow rate for up to 2 h. Notice that the injected solution passes through the entire tube and only slowly accumulates on top of the heavier silicate solution. During this sustained injection the copper-based tubes become darker. After completion of the experiment, the tube is extracted, cut to smaller segments, rinsed in water three times, and allowed to dry at room temperature.

Visual inspection of the dried copper-based tubes suggests that the wall thickness increases with increasing injection time t.

Department of Chemistry and Biochemistry, Florida State University, Tallahassee, Fl 32306-4390, USA. E-mail: steinbck@chem.fsu.edu; Fax: (+1) 850 644 8281; Tel: (+1) 850 644 4824

† Electronic supplementary information (ESI) available: experimental details, additional SEM images and EDS data. See DOI: 10.1039/c1cp22556a

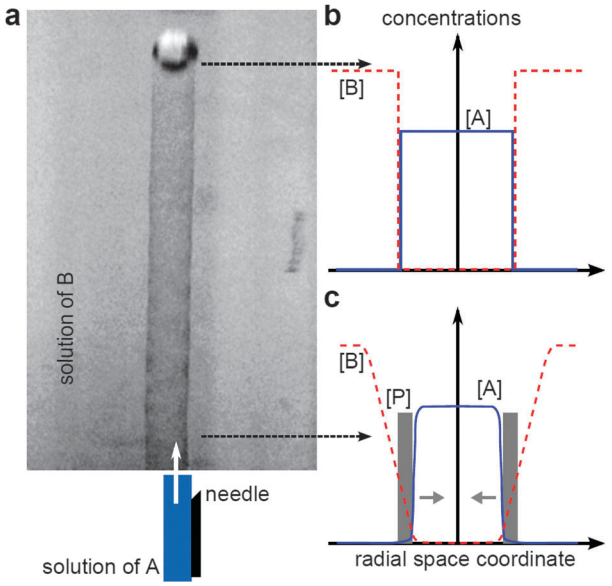

Fig. 1 (a) Schematics of the experimental setup. A precipitation tube forms if solution of A (0.5 M $CuSO_4$ or $ZnSO_4$) is injected into solution of B (sodium silicate). Gas injection through a needle creates a bubble which can pin to the growing tube. The image shows an optical micrograph of a forming tube with an outer radius of 230 μm. (b,c) Schematics of the probable concentration profiles during the onset of reaction (b) and after formation of a precipitate P (c).

This qualitative result is confirmed by scanning electron microscopy (SEM). Two representative examples are shown in Fig. 2. The tube in Fig. 2a is prepared without additional injection ($t = 0$) and has an average wall thickness w of about 5 μm. Injection for $t = 60$ min yields thicker samples with $w \approx 60$ μm (Fig. 2b).

Due to the rough surface texture of the tubes, SEM data yield only approximate values for the wall thickness. We therefore analyze the nonlocal quantity ρw in which ρ denotes the average density of the dried samples. This quantity is measured from the sample's mass (m), length (l), and outer diameter (d) according to $\rho w = m/(l\pi d)$. Notice that the volume of the tube wall is approximated as $wl\pi d$. Typical tube fragments have lengths of 4–14 mm, diameters of 280–750 μm and masses of 30–3000 μg.

The specific ρw kinetics yield important insights into the underlying growth mechanism. For $CuSO_4$ injection we find that the data are well described by square root functions of the form $\sqrt{a(t - t_0)}$ (see Fig. 3 and Table 1). This time dependence suggests that wall growth is a diffusion driven process. The process is controlled by an effective diffusion coefficient D that we obtain from the fits using the relation $D = a/\rho^2$ assuming $\rho = 1.6$ g cm^{-3} which is an average obtained from SEM measurements of w. The data in Table 1 show that D is three orders of magnitude smaller than the diffusion coefficient of small ions in water. The rather small t_0 values average to 17 s and might be related to the initial period of rapid tube formation. We note that all results are widely independent of the outer tube radius. For technical reasons, we did not investigate possible differences between the width of hydrated and dry tube walls.

Another important finding is that the outer diameter of the tube does *not* increase during sustained injection. Consequently the tube wall grows strictly in an inward direction. This surprising result suggests that the outward-directed flux of hydrogen (and copper) ions must be negligible or all together absent. This finding is consistent with results from energy-dispersive X-ray spectroscopy (EDS), which show that the silicon content of the outer wall surface is very low (<10%; see Supporting Information†).

One possible explanation for this unidirectional growth is that the wall is positively charged. For example Bähr *et al.* found that permeation of hydroxide ions in $BaSO_4$ membranes is four times higher than that of hydrogen ions.[22] However, this effect would need to be much stronger in our system to explain the absence of any measurable growth in outward direction. A more relevant and likely explanation is the presence of a propagating reaction-diffusion front. Gálfi and Rácz analyzed such a front in the simple second-order reaction A + B → P.[23] In their analysis, A and B diffuse with equal diffusion coefficients D_i and the initial conditions confine the reactants to separates halves of the medium at constant concentrations $[A]_0$ and $[B]_0$. A similar situation is shown in Fig. 1b. The resulting precipitation front moves exclusively in the direction of the lower initial concentration. Theoretical

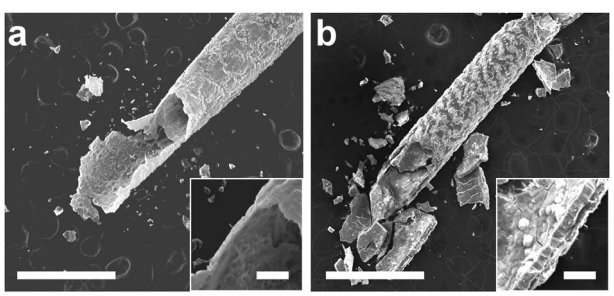

Fig. 2 Scanning electron micrographs of copper-based silica tubes prepared in 1.0 M silicate solution. (a) $t = 0$ min (immediately after tube formation), (b) $t = 60$ min. Insets show the magnified wall. Scale bars: 1 mm, insets 0.1 mm.

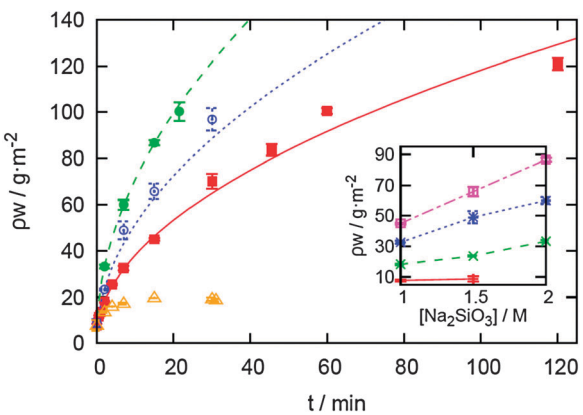

Fig. 3 Measurement of the product of the average wall density ρ and width w as a function of the injection time t. Squares, open circles, and filled circles are data from copper-based tubes prepared in 1.0, 1.5 and 2.0 M sodium silicate solutions, respectively. The lines are fitted square root functions. Triangles denote data from zinc-based tubes (1.0 M silicate). Inset: ρw values of copper-based tubes as a function of sodium silicate concentration. The different data sets correspond to $t = 0$, 2, 7, and 15 min in the order of increasing ρw.

Table 1 Fitting results and effective diffusion constants for the wall growth kinetics of copper-based tubes

$[Na_2SiO_3]$/M	t_0/min	a/g^2 m^{-4} min^{-1}	D/cm^2 s^{-1}
1.0	0.43 ± 0.08	139.0 ± 4.6	0.9×10^{-8}
1.5	0.18 ± 0.14	260.4 ± 19.3	1.7×10^{-8}
2.0	0.25 ± 0.08	490.6 ± 7.8	3.2×10^{-8}

analyses show that the front position is given by $\sqrt{aD_i t}$ where αD_i is an effective diffusion coefficient. The parameter α depends only on $[A]_0/[B]_0$ and is always larger than one.

The key results of this analysis are in excellent agreement with our observations. The model species A and B are best assigned to the protons and hydroxide ions from the acidic copper sulfate and the basic silicate solutions, respectively. This interpretation also explains the increasing rate of wall thickening with increasing concentration of sodium silicate (Fig. 3) as the pH of the solution slightly increases with silicate concentration, thus, amplifying the flux of hydroxide ion into the tube. However, we note that the model does not explicitly include Cu^{2+} ion although it is needed for the precipitation of the main wall-forming compound $Cu(OH)_2$. In addition, the diffusion coefficients of the reactant species are not equal. Nonetheless one can speculate that the low magnitude of the effective diffusion coefficients in Table 1 is not due to a value of α much smaller than one but rather due to slow and/or inhomogeneous ionic transport within the forming wall. Clearly more detailed models are needed to describe the reaction events in a chemically more satisfactory way.

The data in Fig. 3 also reveal a striking difference in the behavior of copper and zinc based tubes: the latter have ρw values that cannot be described by a square-root function but rather saturate at a relatively small value (equivalent to 15 μm). Moreover zinc-based tubes dissolve within approximately 10 min if left in the silicate solution without continued injection of $ZnSO_4$; copper-based tubes, however, do not change if the injection of $CuSO_4$ is stopped. These findings are surprising because–based on our discussion–one should expect the growth kinetics to be widely independent from the employed metal ion. However this anomaly can be explained by considering the amphoteric character of zinc hydroxide, which renders it soluble at pH values[24] higher than 11 (as well as in acidic medium). The measured saturation value (Fig. 3) is hence likely to be the result of a stationary, reaction-transport controlled pH gradient in close vicinity of the tube's interior wall. A description of this gradient is further complicated by the formation of ZnO. The latter oxide is clearly present in dried tubes formed for $t > 2$ min as those samples show a characteristic orange luminescence[25] if excited by ultraviolet light.

Our results suggest the possible synthesis of structures in which the wall consists of several layers of distinct materials. To demonstrate the feasibility of such experiments, we first inject 0.5 M copper sulfate solution into 1.0 M sodium silicate solution for about 20 min. We then switch the injected solution to 0.5 M zinc sulfate and continue injection for about 25 min. Visual inspection of the resulting tube reveals a white layer of precipitate on the inner surface of a blue wall. SEM-EDS measurements of a representative sample are given in Fig. 4. The micrograph in (a) shows a cross-section of the tube wall, in which the outer (inner) surface extends in horizontal direction close to the top (bottom) edge of the frame. The image suggests the presence of two layers. This observation is confirmed by the corresponding EDS profiles in (b). The ordinate denotes the radial space coordinate across the wall with the tick pair marking the approximate positions of the inner and outer wall surface. The abscissa represents the EDS intensities averaged in perpendicular direction (*i.e.* along the wall). The total concentrations in the analyzed area correspond to 49.0, 47.5, 2.3, and 1.2 wt% for Cu, Zn, Si, and S, respectively. The data further reveal that the outer layer is rich in copper while the inner one is rich in zinc. The copper and silicon profiles are tightly correlated although the latter decays more rapidly for decreasing radii. Notice that the overlap of the copper and zinc profiles might be due to Taylor-dispersive mixing of the two solutions in the injection system and the precipitation tube.

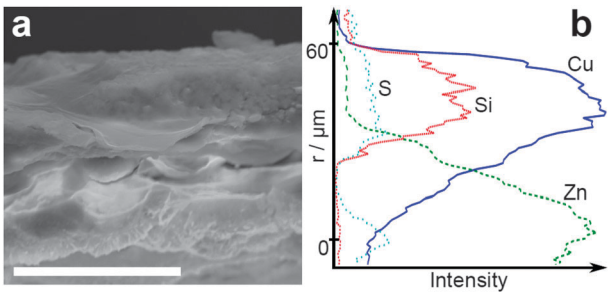

Fig. 4 (a) SEM micrograph of a layered tube wall produced by consecutive injection of Cu^{2+} and Zn^{2+} solution. Scale bar: 50 μm. (b) Elemental distribution across the wall obtained by horizontal averaging of the EDS map of the micrograph in (a). The tick marks in (b) denote the approximate positions of the inner and outer wall surface. Vertical space coordinates in (a) and (b) are matched to allow a direct comparison of the data.

In conclusion, our results reveal that radial wall growth is controlled by a propagating reaction-diffusion front or, in the case of amphoteric species, a stationary pH profile. Future work should explore the material features of multi-layered, composite tube structures and develop more detailed reaction-transport models.

This work was supported by the National Science Foundation (grant no. 1005861).

References

1 B. A. Grzybowski, *Chemistry in motion: reaction-diffusion systems for micro- and nanotechnology*, John Wiley and Sons, Chichester, UK, 2009.
2 A. Sigel, H. Sigel and R. K. O. Sigel, *Biomineralization: From Nature to Application*, John Wiley and Sons, Chichester, UK, 2008.
3 W. W. Smulders and C. W. Jones, and F. J. Schork, *Macromolecules*, 2004, **37**, 9345–9354.
4 D. A. Stone, B. Lewellyn and J. C. Baygents, and R. E. Goldstein, *Langmuir*, 2005, **21**, 10916–10919.
5 R. P. Washington and O. Steinbock, *J. Am. Chem. Soc.*, 2001, **123**, 7933–7934.
6 J. H. E. Cartwright, J. M. García-Ruiz and M. L. Novella, and F. Otálora, *J. Colloid Interface Sci.*, 2002, **256**, 351–359.
7 J. Maselko and P. Strizhak, *J. Phys. Chem. B*, 2004, **108**, 4937–4939.
8 Á. Tóth, D. Horváth, R. Smith, J. R. McMahan and J. Maselko, *J. Phys. Chem. C*, 2007, **111**, 14762–14767.
9 G. J. T. Cooper, A. G. Boulay, P. J. Kitson, C. Ritchie, C. J. Richmond, J. Thiel, D. Gabb, R. Eadie and D.-L. Long, and L. Cronin, *J. Am. Chem. Soc.*, 2011, **133**, 5947–5954.
10 S. Thouvenel-Romans and J. J. Pagano, and O. Steinbock, *Phys. Chem. Chem. Phys.*, 2005, **7**, 2610–2615.

11 R. Makki, M. Al-Humiari, S. Dutta and O. Steinbock, *Angew. Chem., Int. Ed.*, 2009, **48**, 8752–8756.
12 D. A. Stone and R. E. Goldstein, *Proc. Natl. Acad. Sci. U. S. A.*, 2004, **101**, 11537–11541.
13 J. J. Pagano, S. Thouvenel-Romans and O. Steinbock, *Phys. Chem. Chem. Phys.*, 2007, **9**, 110–118.
14 C. Collins, W. Zhou, A. L. Mackay and J. Klinowski, *Chem. Phys. Lett.*, 1998, **286**, 88–92.
15 C. Collins, G. Mann, E. Hoppe, T. Duggal, T. L. Barr and J. Klinowski, *Phys. Chem. Chem. Phys.*, 1999, **1**, 3685–3687.
16 J. J. Pagano, T. Bánsági Jr. and O. Steinbock, *Angew. Chem., Int. Ed.*, 2008, **47**, 9900–9903.
17 G. J. T. Cooper and L. Cronin, *J. Am. Chem. Soc.*, 2009, **131**, 8368–8369.
18 W. Martin, J. Baross, D. Kelley and M. J. Russell, *Nat. Rev. Microbiol.*, 2008, **6**, 805–814.
19 S. Thouvenel-Romans, W. van Saarloos and O. Steinbock, *Europhys. Lett.*, 2004, **67**, 42–48.
20 S. Thouvenel-Romans and O. Steinbock, *J. Am. Chem. Soc.*, 2003, **125**, 4338–4341.
21 J. Pantaleone, Á. Tóth, D. Horváth, L. RoseFigura, W. Morgan and J. Maselko, *Phys. Rev. E: Stat., Nonlinear, Soft Matter Phys.*, 2009, **79**, 056221.
22 G. Bähr, A. Ayalon, F. D. Rompf and P. Hirsch-Ayalon, *J. Membr. Sci.*, 1984, **20**, 103–111.
23 L. Gálfi and Z. Rácz, *Phys. Rev. A: At., Mol., Opt. Phys.*, 1988, **38**, 3151–3154.
24 R. A. Reichle, K. G. McCurdy and L. G. Hepler, *Can. J. Chem.*, 1975, **53**, 3841–3845.
25 S. A. Studenikin and N. Golego, and M. Cocivera, *J. Appl. Phys.*, 1998, **84**, 2287–2294.